

1 Using approximate Bayesian computation to quantify cell-cell
2 adhesion parameters in a cell migratory process

3 Robert J. H. Ross ^{*1}, R. E. Baker ^{†1}, Andrew Parker ^{‡1}, M. J. Ford ^{§2}, R. L. Mort ^{¶2},
4 and C. A. Yates ^{||3}

5 ¹Wolfson Centre for Mathematical Biology, Mathematical Institute, University of
6 Oxford, Radcliffe Observatory Quarter, Woodstock Road, Oxford, OX2 6GG

7 ²MRC Human Genetics Unit, MRC IGMM, Western General Hospital, University of
8 Edinburgh, Edinburgh, EH4 2XU

9 ³Centre for Mathematical Biology, Department of Mathematical Sciences, University of
10 Bath, Claverton Down, Bath, BA2 7AY

11 August 24, 2016

12 **Abstract**

13 In this work we implement approximate Bayesian computational methods to improve the
14 design of a wound-healing assay used to quantify cell-cell interactions. This is important as
15 cell-cell interactions, such as adhesion and repulsion, have been shown to play an important
16 role in cell migration. Initially, we demonstrate with a model of an *ideal* experiment that
17 we are able to identify model parameters for agent motility and adhesion, given we choose
18 appropriate summary statistics. Following this, we replace our model of an ideal experiment
19 with a model representative of a practically realisable experiment. We demonstrate that,
20 given the current (and commonly used) experimental set-up, model parameters cannot be
21 accurately identified using approximate Bayesian computation methods. We compare new

*ross@maths.ox.ac.uk

†baker@maths.ox.ac.uk

‡parker@maths.ox.ac.uk

§matthew.ford@ed.ac.uk

¶richard.mort@igmm.ed.ac.uk

||c.yates@bath.ac.uk

22 experimental designs through simulation, and show more accurate identification of model
23 parameters is possible by expanding the size of the domain upon which the experiment
24 is performed, as opposed to increasing the number of experimental repeats. The results
25 presented in this work therefore describe time *and* cost-saving alterations for a commonly
26 performed experiment for identifying cell motility parameters. Moreover, the results pre-
27 sented in this work will be of interest to those concerned with performing experiments that
28 allow for the accurate identification of parameters governing cell migratory processes, espe-
29 cially cell migratory processes in which cell-cell adhesion or repulsion are known to play a
30 significant role.

31 **Keywords:** Cell migration, adhesion, wound-healing, summary statistics, parameter iden-
32 tification, experimental design, approximate Bayesian computation, individual-based model,
33 simulation.

34 1 Introduction

35 Cell-cell interactions are known to play an important role in several cell migration processes.
36 For example, multiple different cell-cell interactions, such as cell-cell signalling and cell-cell ad-
37 hesion [1], have been identified as promoting metastasis in breast cancer. Repulsive interactions
38 mediated via ephrins on the surface of neural crest stem cells are known to coordinate the early
39 stages of melanoblast migration away from the neural tube [2]. More fundamentally, it is hy-
40 pothesised that the emergence of cell-cell interactions over one billion years ago helped establish
41 the necessary conditions for multicellular organisms [3].

42
43 A well-established approach for studying cell migration is to construct an individual-based
44 model (IBM) to simulate the cell migratory process of interest [4–8]. Typically, this involves
45 using a computational model to simulate a population of agents on a two-dimensional surface,
46 or in a three-dimensional volume. The agents in the IBM represent cells, and each agent is able
47 to move and interact with other agents in the IBM. In this work we use an IBM to simulate a
48 wound-healing assay¹, an experiment commonly used for studying cell motility [9–11].

49

¹Wound-healing assays are also often referred to as scratch assays.

50 If an IBM is an *effective*² representation of a cell migration process it can be used for a number
51 of purposes. One such purpose for an IBM is to perform *in silico* experiments to test scientific
52 hypotheses. For instance, a recent study used an IBM to demonstrate that a simple mechanism
53 of undirected cell movement and proliferation could account for neural crest stem cell coloni-
54 sation of the developing epidermis in the embryonic mouse [4]. Other studies involving IBMs
55 have tested hypotheses concerning the influence of matrix stiffness and matrix architecture on
56 cell migration [12], and the mechanism by which cranial neural crest stem cells become ‘leaders’
57 or ‘followers’ in the embryonic chick to allow their collective migration [6–8].

58

59 IBMs can also be used to *identify* parameters in experimental data (with the caveat that the
60 parameters are model-dependent). The reasoning behind using an IBM to identify parameters
61 in experimental data is as follows: if an IBM is an effective representation of an experiment, then
62 the parameter values the IBM requires to reproduce the experimental data may be representa-
63 tive of the parameter values in the biological process that is the focus of the experiment³. For
64 instance, the value of a parameter that describes cell proliferation rate. Even if the parameter
65 values in the parameterised IBM are not representative of the parameter values in the biological
66 process, the parameterised IBM may still be used to make predictions about the process of
67 interest by performing *in silico* experiments, as described above. These predictions can then be
68 experimentally tested.

69

70 Alternatively, if the IBM is an effective representation of an experiment (i.e. the experimental
71 data can be reproduced), but the parameters of the IBM are not identifiable, this may suggest
72 the experiment is not well-designed (that is, if the experiment has been designed to estimate
73 parameters). By parameters not being identifiable it is meant that different parameter values
74 in the IBM can reproduce the same experimental data. If this is the case, the IBM can then be
75 used to suggest improvements to the experiment’s design, namely by altering the IBM design
76 such that the IBM parameters become identifiable. These alterations can then be applied to the
77 experiment to improve parameter identifiability. For example, a recent study using an IBM has

²By an effective representation we mean the IBM captures the salient features of the process of interest, and is therefore a viable research tool with which to study the process of interest.

³Throughout this work we assume that cellular processes such as migration have constant parameter values associated with them.

78 examined the time-points at which data should be collected from an experiment to maximise
79 the identifiability of IBM parameters [11]. Other theoretical work has shown how to maximise
80 the information content of an experiment by choosing an appropriate experimental design [13].

81

82 The focus of our study is to determine the experimental conditions, and experimental data,
83 required for the accurate identification of cell motility and adhesion parameters in a wound-
84 healing assay. To do so we employ approximate Bayesian computation (ABC), a probabilistic
85 approach whereby a probability distribution for the parameter(s) of interest is generated, as
86 opposed to a point estimate [10, 14, 15]. Although ABC is well-established in some fields, for
87 instance in population genetics [16], its applicability for IBMs representing cell migration is
88 still an area of active research [10, 11]. Recent studies combining ABC and IBMs have been
89 able to identify motility and proliferation rates in cell migratory processes [10], and improve
90 the experimental design of scratch assays [11]. However, as far as we are aware nobody has
91 used ABC methods to examine the experimental conditions, and experimental data, required
92 for the accurate identification of cell motility and adhesion parameters in a wound-healing assay.

93

94 Other methods to identify parameters in experimental data using IBMs also exist. For instance,
95 a standard approach is to generate point estimates of model parameters that best reproduce
96 statistics of the experimental data in the IBM. For example, the generation of motility and
97 proliferation rates for agents in an IBM representing a biological process [4]. This approach,
98 while applicable in some circumstances, often gives no insight into how much uncertainty exists
99 in the parameters chosen, a factor that can be of importance when analysing biological systems.
100 For example, relationships between parameter uncertainty and system robustness are thought
101 to be connected in biological function at a systems level [17].

102

103 The outline of this work is as follows: in Section 2 we introduce the IBM and define the
104 cell-cell interactions we implement. We also outline the method of ABC, and the summary
105 statistics we use to analyse the IBM output. In Section 3 we present results and demonstrate
106 that, given an IBM representing an ideal experiment, we are able to identify IBM parameters
107 for agent motility and adhesion. Following this, we replace our IBM representing an ideal exper-

108 iment with an IBM that simulates a practically realisable experiment. In doing so we show that
109 parameters cannot be successfully identified using ABC given the current experimental design.
110 To improve parameter identifiability we compare different experimental designs, and show that
111 identification of IBM parameters is made more accurate if the size of the domain upon which
112 the experiment is performed is expanded, as opposed to increasing the number of experimental
113 repeats. Experimentally, expanding the size of the domain is equivalent to increasing the field
114 of view of the microscope used to collect the experimental data. For instance, five simulation
115 repeats on a larger domain provides more accurate identification of IBM parameters than 500
116 simulation repeats on a smaller domain. In Section 4 we discuss the results presented in this
117 work.

118 2 Methods

119 In this section we first introduce the IBM. We then define what we mean by summary statistics
120 and explain ABC and its implementation.

121 2.1 Individual-based model

122 An IBM is a computational model for simulating the behaviour of autonomous agents. The
123 agents in the IBM represent cells, and each agent is able to move and interact with other
124 agents. The IBM is simulated on a two-dimensional square lattice with lattice spacing Δ [18]
125 and size L_x by L_y , where L_x is the number of lattice sites in a row, and L_y is the number of
126 sites in a column. Each agent is initially assigned to a lattice site, from which it can move into
127 adjacent sites. If an agent attempts to move into a site that is already occupied by another
128 agent, the movement event is aborted. Processes such as this whereby one agent is allowed per
129 site are often referred to as exclusion processes [18]. In the IBM time evolves continuously, in
130 accordance with the Gillespie algorithm [19], such that agent movement events are modelled as
131 exponentially distributed reaction events in a Markov chain. Attempted agent movement events
132 occur with rate P_m per unit time. $P_m\delta t$, therefore, is the probability of an agent attempting to
133 move in the next infinitesimally small time interval δt . A lattice site is denoted by $v = (i, j)$,
134 where i indicates the column number and j the row number. Each lattice site has four adjacent
135 lattice sites (except for those sites situated on nonperiodic boundaries), and so the number of

136 nearest neighbour lattice sites that are occupied by an agent, denoted by n , is $0 \leq n \leq 4$. We
137 denote the set of unoccupied nearest neighbour lattice sites by \mathcal{U} .

138

139 The IBM domain size for simulations representing ideal experiments is $L_x = 100$ by $L_y = 100$,
140 and the lattice sites indexed by $1 \leq j \leq L_y$ and $1 \leq i \leq 10$, and $1 \leq j \leq L_y$ and $91 \leq i \leq L_x$ are
141 initially occupied by agents. In Fig. 1 the initial conditions in the IBM for the ideal experiment
142 can be seen. The initial condition in Fig. 1 represents a ‘wound’, in that agents are positioned
143 either side of a space, the ‘wound’, that they can migrate into. The agent migration into this
144 space simulates one aspect of the wound-healing process. We refer to this simulation as ideal
145 because the symmetry of the initial conditions may not be possible in a realistic experimental
146 setting. The initial condition is also ideal as it is ‘double-sided’, as opposed to the ‘single-
147 sided’ experiment data that we will later analyse. It has been shown that double-sided initial
148 conditions can provide more information than single-sided initial conditions for some model
149 parameters [11]. For instance, when increasing the number of agents in a simulation improves
150 parameter identifiability.

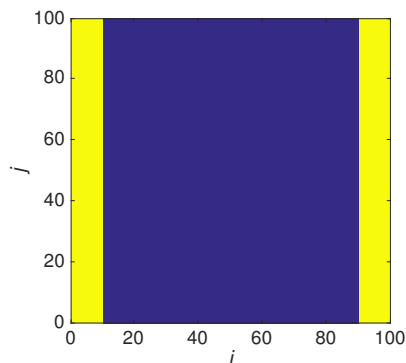


Figure 1: The initial condition in the IBM for the ideal experiment. Yellow indicates a site occupied by an agent and blue indicates an empty lattice site.

151 For the IBM of an ideal experiment all simulations have periodic boundary conditions at the
152 top and bottom of the domain (i.e. for lattice sites indexed by $j = 1$ or $j = L_y$), and no-flux
153 boundary conditions at the left-hand and right-hand boundaries of the domain (i.e. for lattice
154 sites indexed by $i = 1$ or $i = L_x$).

155 2.2 Cell-cell adhesion models

156 In the IBM cell-cell interactions are simulated by altering the probability of an agent attempting
157 to move, depending on the number of nearest occupied neighbours, n , an agent has. We employ
158 two models to simulate cell-cell interactions in the IBM, one of which has been published before
159 [20, 21]. We define $T(v'|v)$ as the transition probability of an agent situated at site v , having
160 been selected to move, attempting to move to site v' , where v' indicates one of the nearest
161 neighbour sites of v . Therefore, $T(v'|v)$ is only non-zero if v and v' are nearest neighbours. The
162 transition probability in the first model, which we refer to as model A, is defined as

$$163 \quad T_A(v'|v) = \frac{1 - n\alpha}{4}, \quad (1)$$

164

165 where α is the adhesion parameter. The subscript A on the transition probability in Eq. (1)
166 indicates that this is the transition probability for model A. If $\alpha > 0$ Eq. (1) models cell-cell
167 adhesion, and if $\alpha < 0$ Eq. (1) models cell-cell repulsion. The transition probabilities stated in
168 Eq. (1) must satisfy

$$169 \quad 0 \leq \sum_{v' \in \mathcal{U}} T_A(v'|v) \leq 1. \quad (2)$$

170

171 Equation (2) ensures the probability of an agent, if selected to move, attempting to move to
172 any of its unoccupied nearest neighbour sites never exceeds unity, and so constrains the value α
173 can take. The transition probability in the second model, which we refer to as model B [20, 21],
174 is defined as

$$175 \quad T_B(v'|v) = \frac{(1 - \alpha)^n}{4}, \quad (3)$$

176

177 and must satisfy

$$178 \quad 0 \leq \sum_{v' \in \mathcal{U}} T_B(v'|v) \leq 1. \quad (4)$$

179

180 As in model A if $\alpha > 0$ Eq. (3) models cell-cell adhesion, and if $\alpha < 0$ Eq. (3) models cell-cell
181 repulsion.

182

183 Models A and B simulate different forms of cell-cell interaction. In model A the transition
184 probability is a linear function of n . Meanwhile, in model B the transition probability is a
185 nonlinear function of n . Not only may these different forms of cell-cell interaction be relevant
186 for different cell types, but implementing two models of cell-cell interaction allows us to test the
187 robustness of the methods we present in this work.

188 **2.3 Summary statistics**

189 Summary statistics are lower-dimensional summaries of data that provide a tractable means to
190 compare different sets of data. Summary statistics are important because experimental data is
191 often of high dimensionality, and if we want to use experimental data to efficiently guide com-
192 putational algorithms we require ways to accurately summarise it. We now define the summary
193 statistics we apply to the IBM output and experimental data. Following this we describe how
194 we utilise these summary statistics to implement ABC.

195

196 We initially use three summary statistics to evaluate the IBM output, all of which have been
197 considered previously [9, 22]. The reason we study three summary statistics is to ascertain
198 which summary statistic is most effective for the identification of agent motility and adhesion
199 parameters in the IBM. These summary statistics are as follows:

200 **Average horizontal displacement of agents**

201 The average horizontal displacement of all agents, \bar{i} , in a given time interval, $[t_i, t_f]$, in the IBM
202 is calculated as

$$203 \quad \bar{i} = \frac{1}{N} \sum_{k=1}^N |i_{t_i}^k - i_{t_f}^k|, \quad (5)$$

204

205 where \bar{i} is the average horizontal displacement of agents, N is the total number of agents in the
206 simulation, $i_{t_i}^k$ is the column position of agent k at time t_i , and $i_{t_f}^k$ is the column position of
207 agent k at time t_f . We only look at the horizontal displacement of agents as this is the direction
208 in which the majority of agent displacement will occur, due to the initial conditions of the IBM
209 (Fig. 1). It has previously been shown that different cell-cell interactions have different effects

210 on the average displacement of agents in an IBM [21]. As may be expected, repulsive (adhesive)
211 interactions between agents tend to increase (decrease) the average displacement of agents, and
212 so the average displacement of agents may be a useful summary statistic for distinguishing
213 between repulsive and adhesive cell-cell interactions in the IBM.

214 **Agent density profile**

215 The agent density profile at time t in the IBM is calculated as:

$$216 \quad C_t(i) = \frac{1}{L_y} \sum_{j=1}^{L_y} \mathbb{1}\{v\}. \quad (6)$$

217

218 Here $C_t(i)$ is the agent density profile and $\mathbb{1}$ is the indicator function for the occupancy of a
219 lattice site v (i.e. 1 if an agent occupies lattice site v , and 0 if it is not occupied by an agent).
220 We have shown previously that different cell-cell interactions have different effects on the agent
221 density profile [21]. For instance, repulsive interactions between agents can create a concave
222 agent density profile, whereas adhesive interactions between agents can create a convex agent
223 density profile. Therefore, the agent density profile may be an effective summary statistic for
224 distinguishing between repulsive and adhesive cell-cell interactions in the IBM.

225 **Pairwise-correlation function**

226 The final summary statistic we consider is the pairwise-correlation function (PCF). The PCF
227 provides a measure of the spatial clustering between agents in an IBM, and has been used
228 frequently in the analysis of cell migratory processes [4, 9, 23, 24]. The PCF has also been
229 successfully used as a summary statistic for the parameterisation of IBMs of cell migration [10].
230 We use i_t^k to denote the column position of agent k at time t , i_t^l to denote the column position
231 of agent l at time t , and define $c_t(m)$ to be the number of occupied pairs of lattice sites for each
232 *nonperiodic*⁴ horizontal pair distance $m = 1, \dots, L_x - 1$ at time t . This means $c_t(m)$ is given by

$$233 \quad c_t(m) = \sum_{k=1}^N \sum_{l=k+1}^N \mathbb{1}\{|i_t^k - i_t^l| = m\}, \quad \forall m = 1, \dots, L_x - 1, \quad (7)$$

234

⁴By nonperiodic it is meant the distance measured between two agents cannot cross the IBM boundary.

235 where $\mathbb{1}$ is the indicator function such that it is equal to 1 if $|i_t^k - i_t^l| = m$, and is equal to
236 0 otherwise. In Eq. (7) only the pair agent distances in the horizontal direction are counted.
237 Given the translational invariance of the initial conditions in the vertical direction of the IBM,
238 the majority of important spatial information will be in the horizontal direction⁵. Binder
239 and Simpson [24] demonstrated that is necessary to normalise Eq. (7) to account for volume
240 exclusion. The normalisation term is

$$241 \quad \hat{c}_t(m) = L_y^2(L_x - m)\rho\hat{\rho}, \quad \forall m = 1, \dots, L_x - 1, \quad (8)$$

243 where $\rho = N/(L_x L_y)$, and $\hat{\rho} = (N - 1)/(L_x L_y - 1)$. Equation (8) describes the expected number
244 of pairs of occupied lattice sites, for each nonperiodic horizontal pair distance m , in an agent
245 population distributed uniformly at random on the IBM domain. Combining Eqs. (7) and (8),
246 the PCF is

$$247 \quad q_t(m) = \frac{c_t(m)}{\hat{c}_t(m)}, \quad (9)$$

249 where $q_t(m)$, the PCF, is a measure of how far $c_t(m)$ departs from describing the expected
250 number of occupied lattice pairs for each horizontal distance of an agent population spatially
251 distributed uniformly at random on the IBM domain.

252 **2.4 Approximate Bayesian computation**

253 Here we introduce our ABC algorithm [14]. We define M as a stochastic model that takes
254 parameters Θ and produces data D . This relationship can be written as $D \sim M(\Theta)$. For the
255 IBM presented in this work $\Theta = (P_m, \alpha)$, where Θ is sampled from a prior distribution, π , and
256 so this relationship can be written as $\Theta \sim \pi$. The relationship between π and Θ is often written
257 as $\Theta \sim \pi(\Theta)$, which indicates that a new Θ sampled from the prior distribution may depend on
258 the previous Θ . This relationship will be relevant later on in this work, however, initially each
259 Θ sampled from π is independent of the previous Θ .

260
261 The identification of IBM parameters in this work centres around the following problem: given

⁵This approach is in agreement with previous studies [24], which showed the most relevant information from the PCF summary statistic is perpendicular to the wound axis in a wound-healing assay.

262 a stochastic model, M , and data, D , what is the probability density function that describes Θ
263 being the model parameters that produced data D ? More formally, we seek to obtain a poste-
264 rior distribution, $p(\Theta|D)$, which is the conditional probability of Θ given D (and the model, M).

265

266 Typically, to compute the posterior distribution a likelihood function, $L(D|\Theta)$, is required.
267 This is because the likelihood function and posterior distribution are related in the following
268 manner by Bayes' theorem:

$$269 \qquad p(\Theta|D) \propto L(D|\Theta)\pi(\Theta). \qquad (10)$$

270

271 That is, the posterior distribution is proportional to the product of the likelihood function and
272 the prior distribution. Approximate Bayesian computation is a well-known method for esti-
273 mating posterior distributions of model parameters in scenarios where the likelihood function
274 is *intractable* [14]. By an intractable likelihood function it is meant that the likelihood function
275 is impossible or computationally prohibitive to obtain.

276

277 In many cases for ABC, due to the high dimensionality of the data, D , it is necessary to
278 utilise a summary statistic, $S = S(D)$. The summary statistics we employ in this work are
279 of varying dimension. For instance, the agent density profile at time t has L_x data points,
280 whereas the average agent displacement at time t has one data point. Therefore we write $S(D)$
281 as $S(D)_{r,t}$, where $S(D)_{r,t}$ is the r^{th} data point in the summary statistic at the t^{th} sampling time.

282

283 The ABC method proceeds in the following manner: we wish to estimate a posterior dis-
284 tribution of Θ given D . We now simulate the process that created D using model M with
285 parameters Θ , sampled from π , and produce data \tilde{D} . We calculate the difference between a
286 summary statistic applied to D and \tilde{D} with

$$287 \qquad d = \sum_{t=1}^T \sum_{r=1}^R |S(D)_{r,t} - S(\tilde{D})_{r,t}|, \qquad (11)$$

288

289 where R is the number of data points in $S(D)$ and T is the number of sampling times. We
290 repeat the above process many times, that is, sample Θ from π , produce \tilde{D} , calculate d with

291 Eq. (11), and only accept Θ for which d is below a user defined certain threshold (alternatively,
292 a predefined number of Θ that minimise d can be accepted). This enables us to generate a
293 distribution for Θ that is an approximation of the posterior distribution, $p(\Theta|D)$, given M .
294 More specific details of the ABC algorithms we implement are introduced when necessary in
295 the text.

296 **3 Results**

297 We begin by demonstrating that for an IBM representing an ideal experiment we are able to
298 identify model parameters, given we use the appropriate summary statistics.

299 **3.1 Ideal experiment**

300 To ascertain the effectiveness of the chosen summary statistics to identify model parameters,
301 we first attempt to identify Θ from data generated *synthetically*. Synthetic data is IBM data
302 generated with fixed parameter values, and so can be thought of as a simulation equivalent of
303 experimental data. To generate the synthetic data using the IBM we proceed as follows:

- 304 1. We choose parameters Θ to identify. To help clarify this explanation let us make these
305 parameters $\Theta = (P_m, \alpha) = (0.5, 0.1)$ in model A⁶.
- 306 2. For model A we perform a simulation of the IBM with $\Theta = (0.5, 0.1)$, generate data,
307 D , and calculate summary statistics, $S(D)$, from the simulation at our time-points of
308 interest. These times are $t = [240, 480, 720]$. We choose these times as they are the
309 times (in minutes) we will later analyse for the simulations of the practically realisable
310 experiment, and correspond to 4 hours, 8 hours and 12 hours into an experiment.
- 311 3. We repeat step 2. ten times and calculate the ensemble average for each summary statistic
312 for each individual time-point.

313 This procedure generates synthetic data for which we will now attempt to identify the param-
314 eters. In this work we present estimates for $P_m = 0.5$ and $\alpha = 0.1$ for model A, and $P_m = 0.5$

⁶A value of $P_m = 0.5$, given that the simulation time will later be defined to be in minutes, and the length of a lattice site represents cell length (typically between 10 μm -100 μm), means that the motility of the agents is biologically realistic. The parameter α is dimensionless. The experimental realism of these parameters will be expanded on when we address the simulation of a practically realisable experiment.

315 and $\alpha = 0.25$, and $P_m = 0.5$ and $\alpha = -0.1$ for model B. We examined identifying further com-
316 binations of values of P_m and α from synthetic data. What we present here is a representative
317 sample of the combinations we tested.

318

319 Throughout this work we sample P_m and α for our model from uniform priors. In the case
320 of model A, $P_m \in [0, 1]$ and $\alpha \in [-0.2, 0.25]$, and for model B, $P_m \in [0, 1]$ and $\alpha \in [-0.2, 1.0]$.
321 We stipulate these lower and upper bounds for α for both models A and B to make sure in-
322 equalities (2) and (4) are satisfied.

323

324 We begin by implementing an ABC rejection algorithm since we expect to identify model
325 parameters quickly as we are simulating an ideal experiment. The rejection ABC algorithm
326 proceeds as follows:

- 327 1. Run 10^4 IBM simulations, in each case using Θ sampled uniformly at random from the
328 prior distributions.
- 329 2. Compute the distance d as defined in Eq. (11) for simulation times $t = [240, 480, 720]$.
- 330 3. Accept the 100 parameter values, Θ , that minimise d .

331 In Fig. 2 the posteriors generated using each of the three summary statistics applied to data
332 from simulations of an ideal experiment are displayed. The most effective summary statistic
333 for identifying the synthetic data parameters is the PCF. The effectiveness of the PCF for pa-
334 rameter identification is evident in the location of the posterior distribution density relative
335 to the red dot (the red dot represents the synthetic data parameter values), and the narrow
336 spread of the posterior distribution density as indicated by the scale bar in Fig. 2 (c), (f) and
337 (i). The agent density profile summary statistic performs less well than the PCF for parameter
338 identification, especially for model A (Fig. 2 (b)). In the case of the average agent displacement
339 many combinations of P_m and α lead to the same average agent displacement, which results
340 in an extended region of possible parameter values. To some extent this is to be expected, as
341 increasing either P_m or α will have opposing effects on the average agent displacement. This
342 means that using agent displacement as a summary statistic results in parameter identifiability
343 issues in this example.

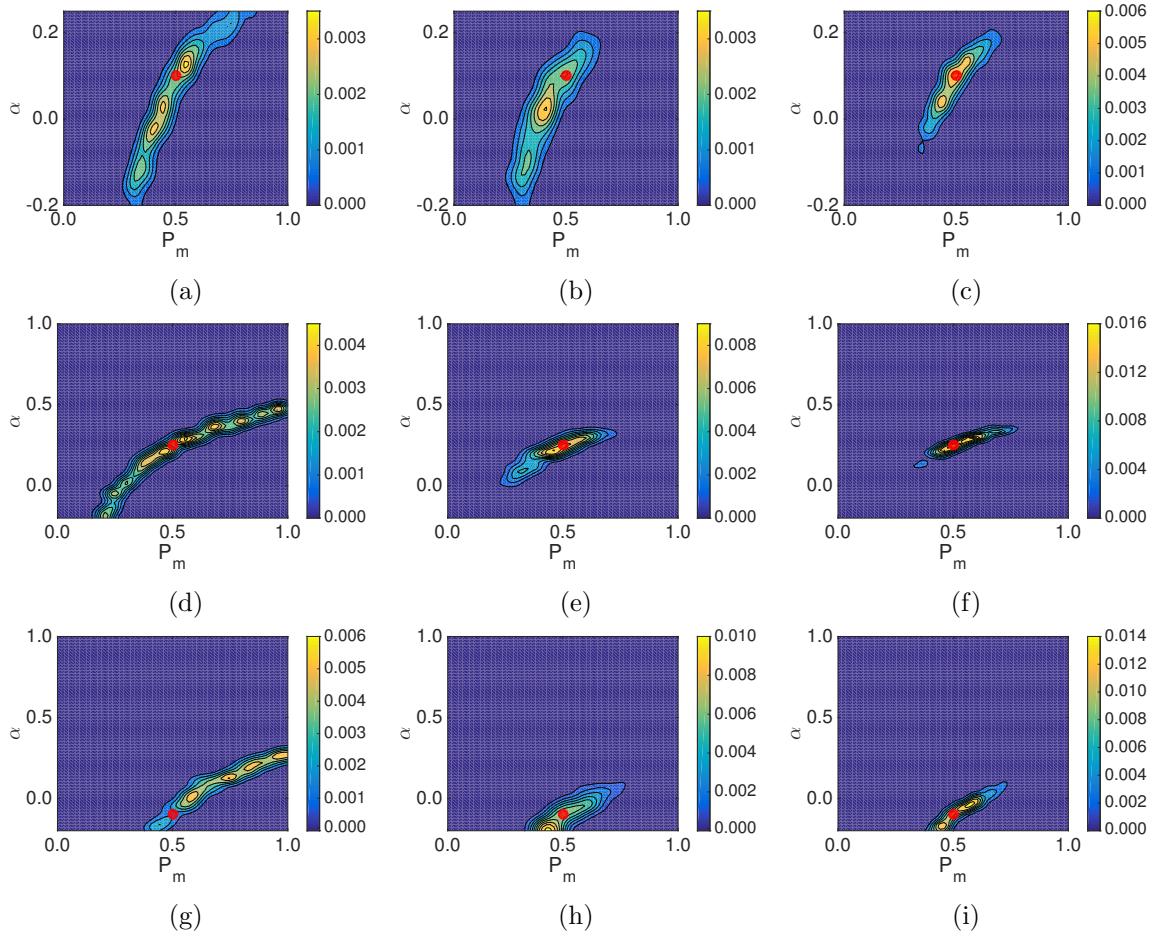


Figure 2: (a)-(c) Posterior distributions for model A for an ideal experiment with different summary statistics: (a) average displacement of agents in the horizontal direction; (b) agent density profile; (c) PCF. In all cases the red dot indicates the value of the parameters used to generate the synthetic data, $P_m = 0.5$, $\alpha = 0.1$. As indicated by the colour bar the yellow regions indicate areas of high relative density of the posterior distribution, while the blue regions indicate areas of low relative density of the posterior distribution. (d)-(f) Model B, $P_m = 0.5$, $\alpha = 0.25$: (d) average displacement of agents in the horizontal direction; (e) agent density profile; (f) PCF. (g)-(i) Model B, $P_m = 0.5$, $\alpha = -0.1$: (g) average displacement of agents in the horizontal direction; (h) agent density profile; (i) PCF.

344

345 To quantify the difference between the performance of the different summary statistics we use
 346 the Kullback-Leibler divergence, which is a measure of the information gained in moving from
 347 the prior distribution to the posterior distribution [25]. The Kullback-Leibler divergence for a
 348 discrete probability distribution is defined as follows:

$$D_{KL}(p|\pi) = \sum_l p(\Theta_l|D) \log \left(\frac{p(\Theta_l|D)}{\pi(\Theta_l)} \right), \quad (12)$$

349

350

351 where the index l accounts for all possible discretised parameter pairs (i.e. all combinations of
352 P_m and α). A larger $D_{KL}(p|\pi)$ value suggests that more information is obtained (the entropy
353 of the distribution is reduced) when moving from the prior distribution to the posterior distri-
354 bution⁷. We discretise our posterior distribution onto a lattice with 2^6 equally spaced values of
355 P_m and 2^6 equally spaced values of α .

356

357 Computing $D_{KL}(p|\pi)$ for all nine plots in Fig. 2 gives: (a) 1.77; (b) 1.70; (c) 2.32; and (d)
358 2.15; (e) 2.57; (f) 3.35; and (g) 2.45; (h) 2.72; (i) 3.27. In tandem with the proximity of the
359 peak of the posterior distribution densities to the red dots in Fig. 2 (c), (f) and (i), compared
360 to Fig. 2 (a)-(b), (d)-(e) and (g)-(h), this suggests that the PCF summary statistic is more
361 effective for parameter identification than the average agent displacement and agent density
362 profile summary statistics.

363 **3.2 Practically realisable experiment**

364 In the previous section we demonstrated that for ideal experimental conditions the PCF sum-
365 mary statistic is best able to identify synthetic data parameters (for an IBM of an ideal ex-
366 periment), and so moving forward we will only use the PCF summary statistic for parameter
367 identification. Previous work has combined summary statistics to improve parameter identifi-
368 cation [10]. However, in this case it makes a negligible improvement to the posterior (results
369 not shown)⁸.

370

371 We now replace our IBM that represents an ideal experiment with an IBM that represents
372 an actual experiment, and examine if synthetic data parameters can be identified in the IBM.
373 We provide brief details of the experiment here, however, a more detailed description can be
374 found in the supplementary material. In Fig. 3 a typical initial frame of the experimental data
375 can be seen.

376

377 In total we have data from five repeats of the experiment. Each data set contains cell track data

⁷However, this does not necessarily mean the posterior distribution is a more accurate representation of the parameter distribution.

⁸That there is little improvement in parameter identification from combining summary statistics is to be expected. Combining summary statistics is most effective when the posterior distributions are ‘orthogonal’, which is not the case for the posterior distributions created by the summary statistics presented here.

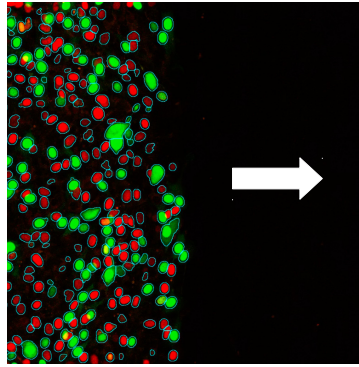


Figure 3: Typical initial frame of the experimental data. The cells are positioned such that they will migrate primarily horizontally into the space without cells, this space represents a wound (the direction of migration is indicated by the white arrow). The red and green cells are the same cells, with red and green indicating which phase of the cell cycle cells are in. In this work we do not take the cell cycle into account.

378 for every cell for sixty-four hours imaged at twenty minute intervals. Therefore, we have the
379 information required to apply our summary statistics to the experimental data. More specifi-
380 cally, we have the position of all cells at each time interval so that the PCF may be computed.

381

382 One key difference between the ideal and practically realisable experiments is the size of the
383 domain and, because of this, the number of agents in a simulation. As we have data from five
384 experiments we now generate our synthetic data from five repeats of the IBM, using the same
385 procedure as described in Section 3.1.

386

387 The experimental images were captured by a microscope with a field of view of $597.24 \mu\text{m}$
388 by $597.24 \mu\text{m}$. The cell size in the experimental images is consistent with each cell occupying a
389 $26 \mu\text{m}$ by $26 \mu\text{m}$ square lattice site. Given the size of the microscope field of view this means
390 the IBM domain size is $L_x = 23$ by $L_y = 23$. We use the average initial conditions from the
391 experiment to generate the initial conditions in the IBM. Exact details of how the initial con-
392 dition is generated in the IBM, and how experimental data is mapped to a lattice can be found
393 in the supplementary material.

394

395 We also alter the IBM to have flux (nonperiodic) boundary conditions at the left-hand and
396 right-hand boundaries of the domain (i.e. for lattice sites with $j = 1$ or $j = N_y$). The left-most
397 column is kept at or above a constant density throughout the simulation time course. That is,

398 after any movement event from the left-most column in the simulation the column density of
399 the left-most column is calculated, and if found to be below a certain density agents are added
400 to empty sites in this column chosen uniformly at random until the required density is achieved.
401 This mechanism ensures that the agent density profile in the IBM replicates the evolution of
402 the experimental data throughout the simulation. Further details regarding the implementation
403 of this boundary condition are provided in the supplementary material. The top and bottom
404 boundaries of the IBM domain remain periodic as cells were seen to move in and out of the
405 microscope field at these boundaries in the experimental images, at an approximately equal rate.

406
407 To reduce the computational time of the ABC algorithm we now employ the Metropolis-Hastings
408 algorithm. We do not implement rejection ABC as we expect parameter identification to be less
409 efficient with a more realistic model, and so we implement a sequential Monte Carlo method.
410 Given our model assumptions our implementation of the Metropolis-Hastings algorithm reduces
411 to a Markov chain Monte Carlo method with a correlated outcome [14], of which we attempt
412 10^6 realisations. Details of the implementation of the algorithm are given in the supplementary
413 material. As before we sample from uniform priors $P_m \in [0, 1]$ and $\alpha \in [-0.2, 0.25]$ for model A,
414 and $P_m \in [0, 1]$ and $\alpha \in [-0.2, 1.0]$ for model B, and collect simulation data at $t = [240, 480, 720]$.
415 We collect simulation data at three time-points so that the computational time is of practical
416 length (our longest ABC implementations took approximately 192 hours). A value of $P_m = 0.5$,
417 given that the simulation time is in minutes, and the length of a lattice site is $26 \mu\text{m}$, means
418 that the motility of the agents is biologically realistic. To be precise, the agents here are ap-
419 proximately five times faster than cell motility rates previously published [4, 9]⁹. However, the
420 cells considered in [4, 9] are not thought to exhibit cell-cell adhesion, and so a higher motility
421 rate is sensible as agent movement is being reduced in the case of cell-cell adhesion in our IBM.

422
423 In Fig. 4 it can be seen that the synthetic data parameters cannot be accurately identified
424 using our ABC method, with the PCF summary statistic, given the current IBM design. This
425 is evident in the location of the red dots relative to the posterior distributions, and the wide
426 spread of the posterior distributions as indicated by the scale bar in Fig. 4. A possible reason
427 why the synthetic data parameters cannot be identified is that the synthetic data does not

⁹Using the relationship that the diffusion coefficient is equal to $P_m \Delta^2$.

428 accurately represent the parameter values used to generate it, making parameter identification
429 infeasible. To examine this possibility we calculated the variance in the PCF synthetic data¹⁰.
430 In Fig. 5 (a)-(c) the blue line indicates the variance in the PCF synthetic data for the current
431 simulation design generated from five repeats of the IBM on a domain of size $L_x = 23$ by
 $L_y = 23$.

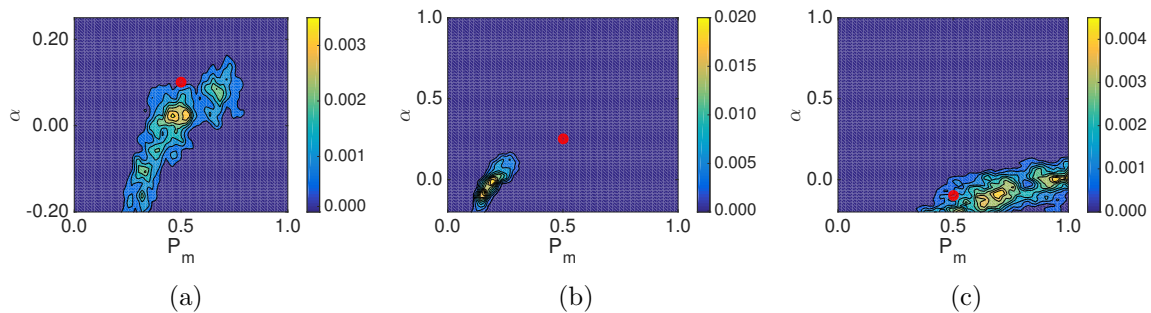


Figure 4: Posterior distributions for simulations of the experiment described in Section 2.5 using the PCF as a summary statistic for an IBM of size $L_x = 23$ and $L_y = 23$. The synthetic data is generated from five repeats of the IBM. (a) Model A: $P_m = 0.5$, $\alpha = 0.1$, (b) model B: $P_m = 0.5$, $\alpha = 0.25$, (c) model B: $P_m = 0.5$, $\alpha = -0.1$. In all cases the red dot indicates the value of the parameters used to generate synthetic data.

432

433

434 If the variance in the summary statistics of the synthetic data precludes accurate identifica-
435 tion of model parameters using ABC, a sensible strategy may be to examine methods to reduce
436 the variance in the summary statistics of the synthetic data. Reducing the variance of the
437 summary statistics may mean the synthetic data is a more accurate reflection of the parameters
438 values used to generate it. This may also explain why parameter identification for the ideal
439 experiment was successful, as the variance in the summary statistics of the synthetic data was
440 much smaller than for the practically realisable experiment (data not shown).

441

442 We conjectured that the variance in the summary statistics of the synthetic data could be
443 reduced in two ways:

444

1. increasing the number of IBM repeats used to generate the synthetic data;

445

2. increasing the size of the IBM domain while keeping the column density of the initial
446 conditions invariant. An example of this proposed initial condition is given in Fig. 6 (b).

¹⁰The variance was calculated using MATLAB's in-built `var` function.

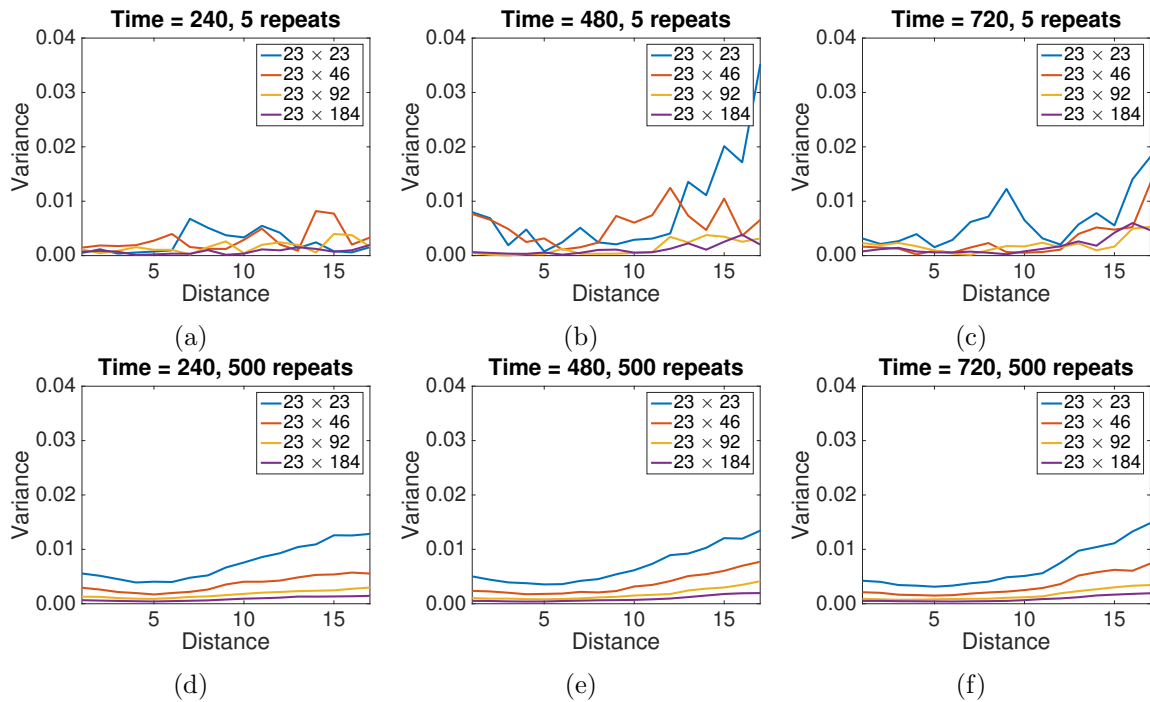


Figure 5: The variance in the PCF synthetic data for model B with $P_m = 0.5$, $\alpha = 0.25$ and different IBM domain sizes. Panels (a)-(c) display synthetic data generated from five repeats of the IBM, panels (d)-(f) display synthetic data generated from 500 repeats of the IBM. The domain size is indicated in the legend.

447 Importantly, increasing the size of the IBM domain increases the number of agents in
 448 the simulation, and can be thought of as equivalent to increasing the field of view of the
 449 microscope.

450 In Fig. 5 the variance in the PCF synthetic data for model B with $P_m = 0.5$ and $\alpha = 0.25$
 451 for different domain sizes and varying numbers of repeats can be seen. It is evident that the
 452 variance in the PCF calculated from 500 repeats of a $L_x = 23$ by $L_y = 23$ sized domain (blue
 453 line in Fig. 5 (d)-(f)) is greater than the variance in the PCF calculated from five repeats of
 454 a $L_x = 23$ by $L_y = 184$ sized domain (purple line in Fig. 5 (a)-(c)). This can be understood
 455 by considering Eq. (7): the number of occupied lattice pairs for each horizontal pair distance
 456 used to generate the PCF does not increase linearly with the number of agents. Specifically,
 457 the number of occupied lattice pairs for each horizontal pair distance that generates the PCF

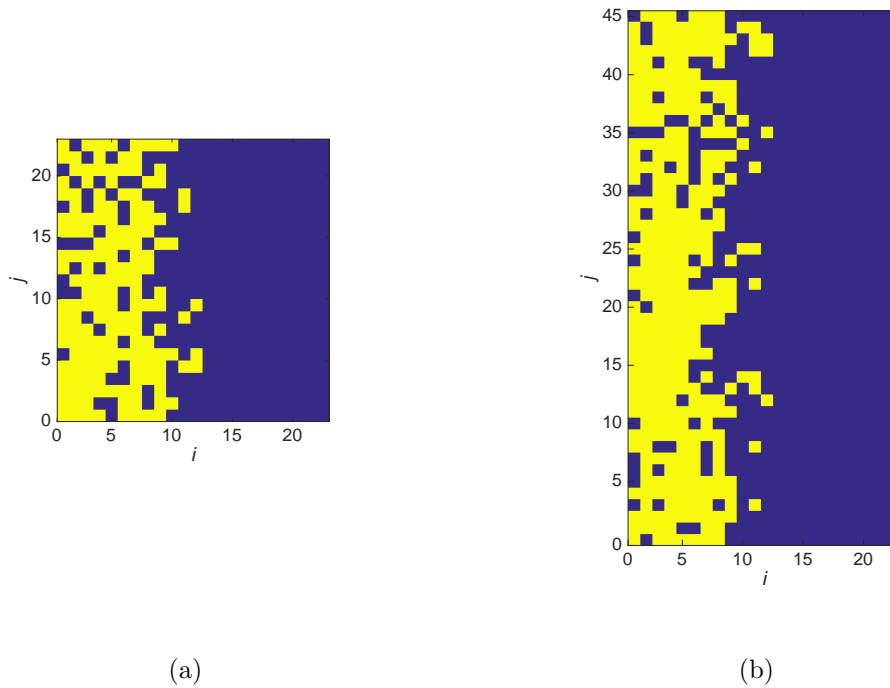


Figure 6: Increasing the size of the simulation domain while keeping the initial column densities the same. Panel (b) is twice the size of panel (a), however, the average initial density of each column is the same for both panels (a) and (b).

458 is proportional to¹¹

459
$$\frac{N(N-1)}{2}. \tag{13}$$

460

461 Therefore, the identification of parameters in experimental data using the PCF as a summary
 462 statistic may be best facilitated by increasing the size of the domain upon which the experiment
 463 is performed, rather than increasing the number of repeats of an experiment with a smaller do-
 464 main. Further variance plots for models A and B for the PCF summary statistic can be found
 465 in the supplementary material.

466

467 It is important to note that it is also the case for the *agent density profile* synthetic data.
 468 If generated from 500 repeats of a $L_x = 23$ by $L_y = 23$ sized domain, the agent density profile
 469 synthetic data will have greater variance than the agent density profile synthetic data generated

¹¹This is not quite correct as a distance of ‘0’ between agents, that is they share the same column, is not accounted for in Eq. (7). To make Eq. (13) exact is not trivial as the expected number of agents each agent shares a column with depends on both the column position and simulation time.

470 from five repeats of a $L_x = 23$ by $L_y = 184$ sized domain (data not shown). In this case it
471 is an artefact of the lattice-based model. This is because the density of each column in the
472 IBM can take on a greater range of values between 0 and 1 as the column length is increased,
473 leading to a reduction in variance in the agent density profile synthetic data (especially in the
474 initial conditions of the simulations used to generate the synthetic data). However, as we do not
475 use the agent density profile summary statistic to identify parameters in the current simulation
476 design we do not pursue this matter further.

477 **3.3 Improving the experimental design**

478 We now confirm that more accurate identification of synthetic data parameters occurs by ex-
479 panding the domain upon which the experiment is performed, as opposed to increasing the
480 number of experimental repeats.

481

482 In Fig. 7 (a)-(c) we plot the posterior distribution for synthetic data generated from 500
483 repeats of a $L_x = 23$ by $L_y = 23$ sized domain, while in Fig. 7 (d)-(f) we plot the posterior
484 distribution generated from synthetic data generated five repeats of a $L_x = 23$ by $L_y = 184$
485 sized domain. As predicted, it is apparent that increasing the domain size is more effective for
486 parameter identification than increasing the number of repeats used to generate the synthetic
487 data. This is evident in the location (and narrow spread) of the posterior distribution relative
488 to the red dot, whereby the posterior distribution is closer to the red dot in the case of Fig.
489 7 (d)-(f) compared to Fig. 7 (a)-(c). Despite this, the identification of the parameters for
490 repulsive interactions remains somewhat elusive (Fig. 7 (f)). A possible reason for this is that
491 the repulsive interaction we present here is a weak one, due to the constraint of Eqs. (2) and
492 (4), and larger values of $|\alpha|$ are easier to identify as they have a more profound effect on the
493 behaviour of the agent population.

494

495 Computing $D_{KL}(p|\pi)$ for all six plots in Fig. 7 gives: (a) 2.55; (b) 2.69; (c) 1.53; and (d)
496 3.69; (e) 2.97; (f) 3.54. In tandem with the proximity of the peak of the posterior distribution
497 densities to the red dots in Fig. 7 (d)-(f) compared to Fig. 7 (a)-(c), this suggests that gener-
498 ating synthetic data on a larger domain is more effective for improving parameter identification

499 than increasing the number of repeats used to generate the synthetic data.

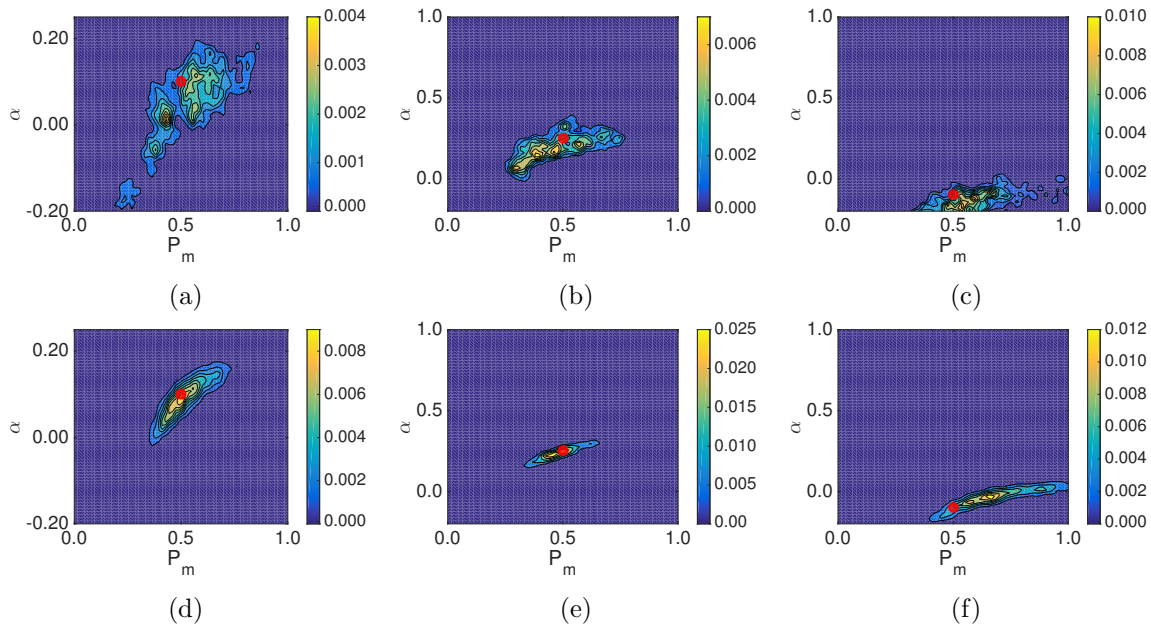


Figure 7: (a)-(c) Posterior distributions for simulations of the experiment using the PCF as a summary statistic for an IBM simulated on a domain of size $L_x = 23$ by $L_y = 23$ with synthetic data generated from 500 repeats. (a) Model A: $P_m = 0.5$, $\alpha = 0.1$, (b) model B: $P_m = 0.5$, $\alpha = 0.25$, (c) model B: $P_m = 0.5$, $\alpha = -0.1$. (d)-(f) Posterior distribution plots for simulations of the experiment using the PCF as a summary statistic for an IBM simulated on a domain of size $L_x = 23$ by $L_y = 184$ with synthetic data generated from five repeats. (a) Model A: $P_m = 0.5$, $\alpha = 0.1$, (b) model B: $P_m = 0.5$, $\alpha = 0.25$, (c) model B: $P_m = 0.5$, $\alpha = -0.1$. Further figure information can be found in Fig. 4.

500 4 Discussion

501 In this work we have presented methods to identify motility and adhesion parameters in an
 502 IBM of a wound-healing assay. Our findings suggest that for a commonly performed exper-
 503 iment increasing the size of the experimental domain can be more effective in improving the
 504 accuracy of parameter identification, when compared to increasing the number of repeats of the
 505 experiment. This is because increasing the size of the domain, which is equivalent to increasing
 506 the number of cells in the experiment, more effectively reduces the variance in the synthetic
 507 data from which the parameters are identified. The reason for this reduction in variance is
 508 explained by Eq. (7), where the number of agent pair counts that generate the PCF increases
 509 nonlinearly with the number of agents on the domain. In addition, increasing the size of the
 510 experimental domain may make the collection of experimental data less time-consuming, as

511 potentially fewer repeats of the experiment will have to be conducted. For instance, five repeats
512 of the experiment on a larger domain provides more information about parameters than 500
513 repeats of the experiment on a smaller domain (in the examples we have presented in this work).

514

515 We also studied using the average horizontal displacement of agents and the agent density
516 profile as summary statistics. These were found to be less effective than the PCF in parameter
517 identification. This was especially the case for the averaged agent displacement, whereby a
518 range of adhesion and motility parameters could result in the same average agent displacement.
519 This result suggests that agent displacement may not be a suitable summary statistic for esti-
520 mating cell motility and adhesion parameters, due to parameter identifiability issues.

521

522 The obvious extension to the work presented here is to experimentally validate the findings.
523 That is, expand the wound-healing experimental domain and demonstrate: i) the cell migratory
524 process can be effectively described by the model we have presented here; and ii) the experi-
525 mental parameters are identifiable with a larger experimental domain. If validated, alterations
526 could be made to the IBM to try and further improve parameter identification, and evidence
527 may be provided that demonstrates which adhesion model, A or B, is more applicable to the
528 cell type under consideration.

529

530 To conclude, the findings presented in this work will be of particular interest to those con-
531 cerned with performing experiments that enable the effective parameterisation of cell migratory
532 processes. In particular, cell migratory processes in which cell-cell adhesion or repulsion are
533 known to play an important role. More generally, we have also suggested time and cost-saving
534 alterations to a commonly performed experiment for identifying cell motility parameters.

535 **Acknowledgements**

536 RJHR would like to thank the UK's Engineering and Physical Sciences Research Council (EP-
537 SRC, EP/G03706X/1) for funding through a studentship at the Systems Biology programme
538 of The University of Oxford's Doctoral Training Centre. RLM was supported by a Medical
539 Research Scotland Project Grant (436FRG). The authors declare no competing interests.

540 Contributions

541 RJHR, REB and CAY conceived the work, and performed the mathematical and computational
542 analysis. Data collection and analysis was performed by RLM and MJF. RJHR, REB and CAY
543 drafted the manuscript. All authors agree with manuscript results and conclusions. All authors
544 approved the final version.

545 References

- 546 [1] K. J. Cheung and A. J. Ewald. Illuminating breast cancer invasion: diverse roles for cell–cell
547 interactions. *Current Opinion in Cell Biology*, 30:99–111, 2014.
- 548 [2] A. Santiago and C. A. Erickson. Ephrin-B ligands play a dual role in the control of neural
549 crest cell migration. *Development*, 129(15):3621–3632, 2002.
- 550 [3] J. J. Fredberg. Power steering, power brakes, and jamming: Evolution of collective cell-cell
551 interactions. *Physiology*, 29(4):218–219, 2014.
- 552 [4] R. L. Mort, R. J. H. Ross, K. J. Hainey, O. Harrison, M. A. Keighren, G. Landini, R. E.
553 Baker, K. J. Painter, I. J. Jackson, and C. A. Yates. Reconciling diverse mammalian
554 pigmentation patterns with a fundamental mathematical model. *Nature Communications*,
555 7(10288), 2016.
- 556 [5] B. J. Binder, K. A. Landman, D. F. Newgreen, J. E. Simkin, Y. Takahashi, and D. Zhang.
557 Spatial analysis of multi-species exclusion processes: application to neural crest cell migra-
558 tion in the embryonic gut. *Bulletin of Mathematical Biology*, 74(2):474–90, 2012.
- 559 [6] R. McLennan, L. Dyson, K. W. Prather, J. A. Morrison, R. E. Baker, P. K. Maini, and
560 P. M. Kulesa. Multiscale mechanisms of cell migration during development: theory and
561 experiment. *Development*, 139(16):2935–2944, 2012.
- 562 [7] R. McLennan, L. J. Schumacher, J. A. Morrison, J. M. Teddy, D. A. Ridenour, A. C. Box,
563 C. L. Semerad, H. Li, W. McDowell, D. Kay, P. K. Maini, R. E. Baker, and P. M. Kulesa.
564 Neural crest migration is driven by a few trailblazer cells with a unique molecular signature
565 narrowly confined to the invasive front. *Development*, 142(11):2014–2025, 2015.

- 566 [8] R. McLennan, L. J. Schumacher, J. A. Morrison, J. M. Teddy, D. A. Ridenour, A. C.
567 Box, C. L. Semerad, H. Li, W. McDowell, D. Kay, P. K. Maini, R. E. Baker, and P. M.
568 Kulesa. VEGF signals induce trailblazer cell identity that drives neural crest migration.
569 *Developmental Biology*, 407(1):12–25, 2015.
- 570 [9] S. T. Johnston, M. J. Simpson, D. L. S. McElwain, B. J. Binder, and J. V. Ross. Interpreting
571 scratch assays using pair density dynamics and approximate Bayesian computation. *Open*
572 *Biology*, 4(9):140097, 2014.
- 573 [10] S. T. Johnston, M. J. Simpson, and D. L. S. McElwain. How much information can be
574 obtained from tracking the position of the leading edge in a scratch assay? *Journal of The*
575 *Royal Society Interface*, 11(97):20140325, 2014.
- 576 [11] S. T. Johnston, J. V. Ross, B. J. Binder, D. L. . McElwain, P. Haridas, and M. J. Simpson.
577 Quantifying the effect of experimental design choices for *in vitro* scratch assays. *Journal*
578 *of Theoretical Biology*, 400:19–31, 2016.
- 579 [12] D. K. Schlüter, I. Ramis-Conde, and M. A. J. Chaplain. Computational modeling of single-
580 cell migration: the leading role of extracellular matrix fibers. *Biophysical Journal*, 103(6):
581 1141–1151, 2012.
- 582 [13] J. Liepe, S. Filippi, M. Komorowski, and M. P. H. Stumpf. Maximizing the information
583 content of experiments in systems biology. *PLoS Computational Biology*, 9(1):e1002888,
584 2013.
- 585 [14] P. Marjoram, J. Molitor, V. Plagnol, and S. Tavaré. Markov chain Monte Carlo without
586 likelihoods. *Proceedings of the National Academy of Sciences*, 100(26):15324–15328, 2003.
- 587 [15] E. van der Vaart, M. A. Beaumont, A. S. A. Johnston, and R. M. Sibly. Calibration and
588 evaluation of individual-based models using Approximate Bayesian Computation. *Ecolog-*
589 *ical Modelling*, 312:182–190, 2015.
- 590 [16] M. A. Beaumont, W. Zhang, and D. J. Balding. Approximate Bayesian Computation in
591 population genetics. *Genetics*, 162(4):2025–2035, 2002.
- 592 [17] H. Kitano. Biological robustness. *Nature Reviews Genetics*, 5(11):826–837, 2004.

- 593 [18] T. M. Liggett. *Stochastic Interacting Systems: Contact, Voter, and Exclusion Processes*.
594 Springer-Verlag, Berlin, 1999.
- 595 [19] D. T. Gillespie. Exact stochastic simulation of coupled chemical reactions. *Journal of*
596 *Physical Chemistry*, 81(25):2340–2361, 1977.
- 597 [20] E. Khain, L. M. Sander, and C. M. Schneider-Mizell. The role of cell-cell adhesion in wound
598 healing. *Journal of Statistical Physics*, 128(1-2):209–218, 2007.
- 599 [21] R. J. H. Ross, C. A. Yates, and R. E. Baker. Inference of cell–cell interactions from
600 population density characteristics and cell trajectories on static and growing domains.
601 *Mathematical Biosciences*, 264:108–118, 2015.
- 602 [22] M. J. Simpson, K. K. Treloar, B. J. Binder, P. Haridas, K. J. Manton, D. I. Leavesley,
603 D. L. S. McElwain, and R. E. Baker. Quantifying the roles of cell motility and cell prolifer-
604 ation in a circular barrier assay. *Journal of The Royal Society Interface*, 10(82):20130007,
605 2013.
- 606 [23] D. J. G. Agnew, J. E. F. Green, T. M. Brown, M. J. Simpson, and B. J. Binder. Distin-
607 guishing between mechanisms of cell aggregation using pair-correlation functions. *Journal*
608 *of Theoretical Biology*, 352:16–23, 2014.
- 609 [24] B. J. Binder and M. J. Simpson. Quantifying spatial structure in experimental observations
610 and agent-based simulations using pair-correlation functions. *Physical Review E*, 88(2):
611 022705, 2013.
- 612 [25] K. P. Burnham and D. R. Anderson. *Model Selection and Multimodel Inference: A Practical*
613 *Information-Theoretic Approach*. Berlin, Germany: Springer, 2002.